Multipartite classically entangled scalar beams

Zhensong Wan[1,2], **Yijie Shen**[3,4], **Qiang Liu**[1,2,5], **and Xing Fu**[1,2,6]

[1] *Key Laboratory of Photonic Control Technology (Tsinghua University), Ministry of Education, Beijing 100084, China*
[2] *State Key Laboratory of Precision Measurement Technology and Instruments, Department of Precision Instrument, Tsinghua University, Beijing 100084, China*
[3] *Optoelectronics Research Centre, University of Southampton, Southampton SO17 1BJ, UK*
[4] *y.shen@soton.ac.uk*
[5] *qiangliu@mail.tsinghua.edu.cn*
[6] *fuxing@mail.tsinghua.edu.cn*

Compiled May 17, 2022

Classically entangled light used to refer to a class of vector beams with space-polarization non-separable states akin to entangled states, which enable novel quantum-analogue methods and applications in structured light. Here we argue the classical entanglement is not limited in vector beams, but also available for scalar beams. We theoretically and experimentally demonstrate a class of scalar ray-wave structured light with multiple controllable local degrees of freedom (DoFs) to emulate multipartite entangled states, including the Greenberger–Horne–Zeilinger states. Our work unveils a rich parameter space for high-dimensional and multi-DoF control of structured light to extend applications in classical-quantum regimes.

http://dx.doi.org/10.1364/ao.XX.XXXXXX

For a long time, the polarization of photon was the only degree of freedom (DoF) to prepare entangled states in quantum optics. Structured light recently attracted increasing attentions due to its ability to tailor multiple DoFs of light for on-demand patterns [1], especially the vector beams with space-polarization nonseparability, that possess similar forms as non-separable states of quantum entanglement [2–4]. Such classically entangled light enabled numerous quantum-analogue methods to characterize fine-scale beam structure [5, 6], as well as advanced applications such as communication, metrology, and cryptography [7–9]. Moreover, the multipartite classically entangled states were recently created and controlled in novel high-dimensional ray-wave vectorial structured light [10]. However, these classically entangled beams were limited as vector beams.

Indeed, there were some works to emulate entangled states using optical system without vector beams. For instance, one could use classical beam splitting system with modulated optical paths to simulate entangled states, but it was not a paraxial structured beam and the bulky control is very complicated [11, 12]. Recently, orbital angular momentum (OAM) and transverse linear momentum were used as two local DoFs to construct bipartite entangled state, but this approach cannot access multipartite states [13, 14]. It is still a challenge today to create multipartite classically entangled states in paraxial scalar beams.

In this letter, the digital modulation on a class of scalar *ray-wave geometric beam (RWGB)* is used to access new controllable DoFs and create quantum-like nonseparable states. Specifically, we exploit five intrinsic DoFs embedded in the RWGB that is both wave-like and ray-like, to realize multipartite high-dimensional classically entangled light. We experimentally demonstrate fully controllable tripartite entangled states in eight-dimensional space by three DoFs (oscillating direction, roundtrip location and central OAM), including the complete set of classical Greenberger–Horne–Zeilinger (GHZ) states. Furthermore, the extension mechanism for even higher-dimensional multipartite classical entanglement is illustrated by introducing the sub-OAM DoF and ray oscillating phase DoF.

Concept. To explore the approach of generating and controlling scalar classical GHZ state, we exploit the multiple DoFs of RWGBs. Such geometric beams are carefully crafted spatial modes that can always be coupled to a special ray caustics. The behaviour of the geometric beams can be described by both geometric rays and wave diffraction, leading to more controllable DoFs than conventional spatial modes [15]. In the ray-like picture, the states of rays fulfil a ballistic geometry bouncing back-and-forth in a cavity, that can be described by two DoFs, i.e. ray oscillating direction ($|+\rangle$ and $|-\rangle$) and roundtrip location ($|1\rangle$ and $|2\rangle$), as shown in Fig. 1(a). On the other hand, in the wave-like picture, the coherent laser beam can be imbued with typical wave features such as OAM. Figure 1 (c) illustrates the examples of RWGBs carrying positive and negative OAM ($|+\ell\rangle$ and $|-\ell\rangle$), that are coupled with right- and left-handed twisted ray caustics, respectively. In addition to these three DoFs, more DoFs can be utilized. For example, the ray oscillating phase $|\phi\rangle$ determines the orientation of the wave-packet, and sub-OAM DoF $|m\rangle$ controls the OAM in each ray, as detailed in Supplement 1. Notably, these RWGBs are generated in this work by the digital computer generated hologram (CGH) modulation method with a spatial light modulator (SLM) [16], as shown in Fig. 1(b), enjoying much higher flexibility of beam tailoring and tuning, compared with the traditional cavity oscillating method (Fig. 1(a)).

Hereinafter, three DoFs including central OAM, ray oscillating direction and roundtrip location are utilized to create a classically tripartite entangled light. We employ two scalar RWGBs in an eight-dimensional Hilbert space spanned by the basis states

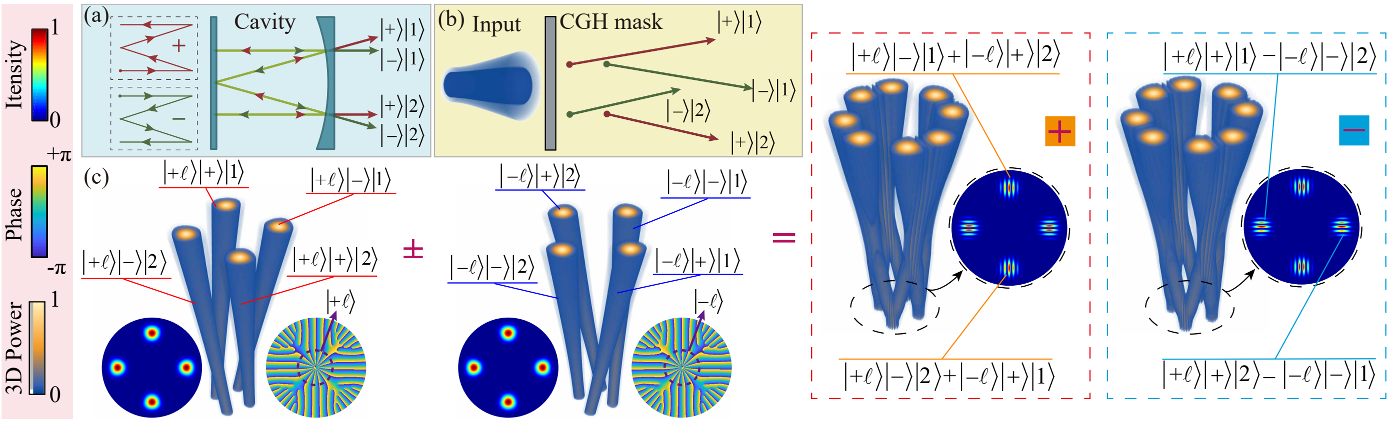

Fig. 1. Concept of multipartite classically entangled scalar RWGBs. (a) Illustration of oscillation direction states, $|+\rangle$ and $|-\rangle$, and roundtrip location, $|1\rangle$ and $|2\rangle$, for describing the geometric rays; (b) cavity oscillation states analogy with digital modulation, as realized by CGH masks in this work; (c) illustration of a new high-dimensional scalar structured light field comprising of multiple intrinsic DoFs in two superposed RWGBs wave-packet (plotted from $z = 0$ to $z = 2f$, where f is the Rayleigh length), which is utilized to construct classical 8-dimensional tripartite entangled states with $|\alpha_i| = \sqrt{2}/4 (i = 1$ to $8)$.

in $|\mathcal{H}_8\rangle \in \{|+\ell\rangle|+\rangle|1\rangle, |+\ell\rangle|+\rangle|2\rangle, |+\ell\rangle|-\rangle|1\rangle, |+\ell\rangle|-\rangle|2\rangle, |-\ell\rangle|+\rangle|1\rangle, |-\ell\rangle|+\rangle|2\rangle, |-\ell\rangle|-\rangle|1\rangle, |-\ell\rangle|-\rangle|2\rangle\}$, in which each ray of these two superposed RWGBs corresponds to a basis state. The full set of states are illustrated in Fig. 1 (c). We externally modulate and engineer the amplitude and phase of each term independently. The tripartite entangled states can be generally expressed as

$$\begin{aligned}|\mathcal{S}_8\rangle = {} & \alpha_1|+\ell\rangle|+\rangle|1\rangle + \alpha_2|+\ell\rangle|-\rangle|1\rangle + \alpha_3|+\ell\rangle|+\rangle|2\rangle \\ & + \alpha_4|+\ell\rangle|-\rangle|2\rangle + \alpha_5|-\ell\rangle|+\rangle|1\rangle + \alpha_6|-\ell\rangle|-\rangle|1\rangle \\ & + \alpha_7|-\ell\rangle|+\rangle|2\rangle + \alpha_8|-\ell\rangle|-\rangle|2\rangle\end{aligned} \quad \textbf{(1)}$$

In particular, we can create each of the eight GHZ basis states from the complete set. For example, when $|\alpha_1| = |\alpha_8| = \sqrt{2}/2$ and all other amplitudes are zero, the corresponding maximally entangled pairs can be obtained by modulating the phase shift between two basis states:

$$|\mathrm{GHZ}_1^{\pm}\rangle = \frac{|+\ell\rangle|+\rangle|1\rangle \pm |-\ell\rangle|-\rangle|2\rangle}{\sqrt{2}} \quad \textbf{(2)}$$

where GHZ_1^+ and GHZ_1^- states are obtained by coherent superposition of the left rays of two RWGBs in Fig. 1 (c) with phase difference of 0 and π, respectively. The other three maximally entangled pairs for tripartite entanglement are given by:

$$\begin{aligned}|\mathrm{GHZ}_2^{\pm}\rangle &= \frac{|+\ell\rangle|-\rangle|1\rangle \pm |-\ell\rangle|+\rangle|2\rangle}{\sqrt{2}} \\ |\mathrm{GHZ}_3^{\pm}\rangle &= \frac{|+\ell\rangle|+\rangle|2\rangle \pm |-\ell\rangle|-\rangle|1\rangle}{\sqrt{2}} \\ |\mathrm{GHZ}_4^{\pm}\rangle &= \frac{|+\ell\rangle|-\rangle|2\rangle \pm |-\ell\rangle|+\rangle|1\rangle}{\sqrt{2}}\end{aligned} \quad \textbf{(3)}$$

Notably, these four GHZ_s^+ $(s = 1, 2, 3, 4)$ states that are spatially non-overlapping can be obtained simultaneously, by coherent superposition of two RWGBs with phase difference of 0. Similarly, four GHZ_s^- $(s = 1, 2, 3, 4)$ states are obtained simultaneously by coherent superposition of these two RWGBs with phase shift of π. The wave-packet of classical 8-dimensional tripartite entangled states for $|\alpha_i| = \sqrt{2}/4 (i = 1$ to $8)$ are shown in the right of Fig. 1 (c).

Experimental setup. The generation and measurement method of arbitrary classical tripartite entangled states, as described by Eq. (1), is demonstrated as follows. As shown in Fig. 2, the beam from a 532 nm diode laser is expanded and collimated, and goes through linear polarizers (LPs) and half-wave plates (HWPs) that are set to control the polarization of light as vertical at the entrance of a reflective SLM, which is loaded with CGH masks and modulates the phase of the wavefront as required. The modulated beam then propagates into a beam reducer composed by two lenses (L3 and L4). An aperture is located in the confocal plane of L3 and L4, transmitting the first diffraction

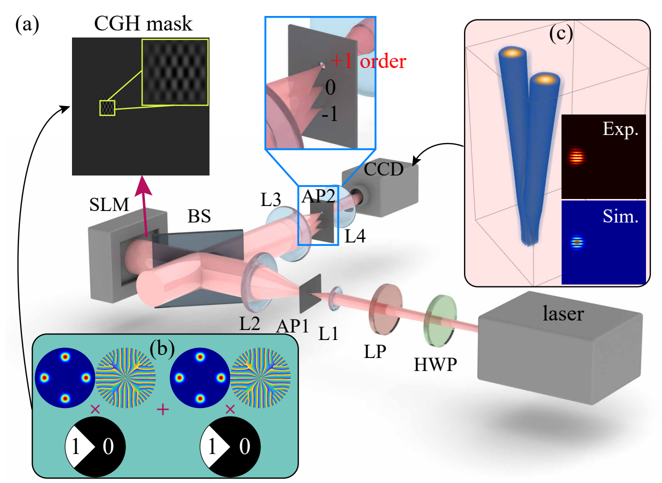

Fig. 2. Schematic diagram. (a) Layout of experimental setup. LP, linear polarizer; HWP, half-wave plate; L1-L4, lens; BS, beam splitter; SLM, spatial light modulator; AP1 and AP2, aperture; CCD, charge-coupled device camera; CGH mask, computer generated holographic mask; (b) design of digital sector aperture; (c) theoretical wave-packet propagation of $|\mathrm{GHZ}_1^+\rangle$ in free space, with insets of experimental and theoretical intensity patterns.

order and blocking all other orders. Finally, the nature of the prepared states is directly measured by a camera. Notably, wave interference happens at ray overlapping region between two scalar RWGBs, and the interference stripes indicate the phase difference between rays. This is the key principle that the RWGB, rather than a common beam without ray-wave duality, can realize higher-dimensional control.

As mentioned above, four GHZ_s^+ (GHZ_s^-) states are generated simultaneously by the superposition of two coherent RWGBs with phase difference of 0 (π). Importantly, these four GHZ states are non-overlapped spatially. To spatially select the desired basis rays, a digital sector aperture is applied, as shown in Fig. 2 (b), to achieve complex amplitude modulation, which allows us to freely control the complex weights of arbitrary basis states in Eq. (1) of a tripartite entangled state. Experimental and theoretical intensity patterns of $\left|\mathrm{GHZ}_1^+\right\rangle$, together with the theoretical wave-packet propagation in free space are shown in Fig. 2 (c). The intensity distribution is a two-lobed structure, consistent with the corresponding GHZ state, while the evolution of the lobe intensities and interferometric fringe patterns confirm the field.

Results and discussions. Hereinafter, a quantum-like state tomography method is presented to measure the experimental GHZ states, keeping in mind that the quantum state tomography is realized by a sequence of projective measurements for estimating full information of quantum states. For a given classical tripartite entangled state as described by Eq. (1), the full information is described as all the eight complex numbers α_1 to α_8 that can't be measured directly. Thus, we measure the amplitude and phase of α_1 to α_8 by the relative power of each basis ray and interference fringes between basis rays, respectively, which can be realized from the propagation profiles of the ray-like wave packets, by post-processing the experimentally captured classical light field patterns in the planes of $z = 0$, $z = f$ and $z = 2f$. On one hand, the eight basis rays are separated in the plane of $z = 2f$ (as shown in Fig. 1), thus the relative amplitude of eight complex coefficients can be obtained by comparing the relative power of each ray. On the other hand, the relative phase can be decided by measuring the correlation degree between the simulated interference fringes patterns and the experimental results in the overlapping interference planes ($z = 0$ and $z = f$) of rays. Since the eight basis states of a tripartite system can be divided into spatially separated four tripartite two-level state pairs in the beam waist plane ($z = 0$), we can find the relative phase of two basis rays where the correlation degree reaches the maximum value. Similarly, the relative phase of basis rays in different two-level state pairs can be calculated from the interference region in the plane of $z = f$. Details about tomographic measurements are provided in Supplement 1.

By the tomographic measurements described above, the complex coefficients of all basis states are ascertained, and hence the tripartite entangled states can be clearly distinguished as Eq. 2. Then the constructed density matrices that fully describe our classical tripartite entangled states can be inferred from the experimental intensity patterns. Each state is calculated from a density matrix of the state, with the results of $\left|\mathrm{GHZ}_1^+\right\rangle$ and $\left|\mathrm{GHZ}_1^-\right\rangle$ shown in Fig. 3 (c) and (d) respectively, while other states are described in Supplement 1. The corresponding theoretical density matrices are shown Fig. 3 (c) and (d), respectively. We find that the theoretical and experimental density matrices are in very good agreement, with the fidelity values as (0.98, 0.99, 0.99, 0.98, 0.99, 0.99, 0.97, 0.99) for GHZ states ($\left|\mathrm{GHZ}_1^\pm\right\rangle$ to $\left|\mathrm{GHZ}_4^\pm\right\rangle$).

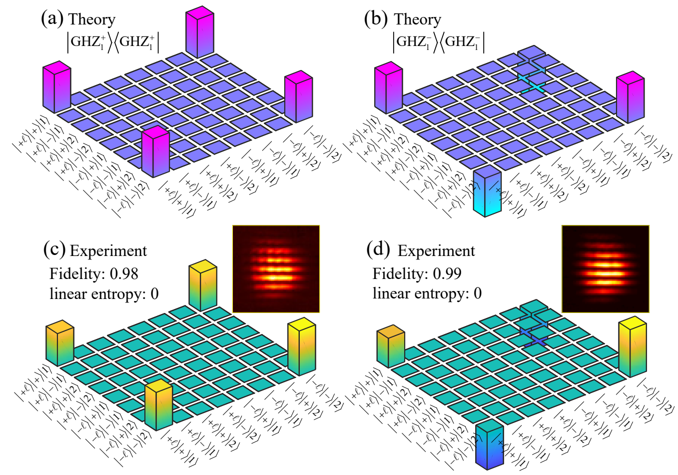

Fig. 3. Density matrices of the tripartite entangled GHZ states. (a) and (b) are the theoretical density matrices of $\left|\mathrm{GHZ}_1^+\right\rangle$ and $\left|\mathrm{GHZ}_1^-\right\rangle$, respectively. (c) and (d) are the real parts of the density matrices for the experimentally obtained $\left|\mathrm{GHZ}_1^+\right\rangle$ and $\left|\mathrm{GHZ}_1^-\right\rangle$, respectively, with the insets of measured intensity pattern.

By now, we have created eight-dimensional tripartite entangled states, by the coherently superimposed two RWGBs utilizing three DoFs. We use RWGB with four rays to demonstrate our scheme, corresponding to four back-and-forth ray trajectories during a mode oscillation period in the cavity, with two oscillation direction states and two roundtrip location states. Combining with central OAM DoF with 2 states ($|+\ell\rangle$ and $|-\ell\rangle$), we can control the structured light in $2 \times 2 \times 2 = 8$ dimensional space. Alternatively, the 8 dimensional space can be realized by replacing DoF of the central OAM $|l\rangle$ by the sub-OAM $|m\rangle$, while the sign of central OAM is related to the sign of the sub-OAM, with two cases of $|+\ell, -m\rangle$ and $|-\ell, +m\rangle$ illustrated in Fig. 4(a). Furthermore, even higher dimensional space can be reached. One way is to adopt the RWGB with more rays. For instance, superposition of two RWGBs, each has 6 back-and-forth ray trajectories in the cavity and thus 3 roundtrip location states, achieve the advanced control in a $2 \times 3 \times 2 = 12$ dimensional space. The basis states in 12-dimensional Hilbert space are represented by each ray of two RWGBs, as shown in Fig. 4(b). Another way is to bring in the intrinsic DoF of ray oscillating phase ($|0\rangle$ and $|\pi\rangle$) and realize four-partite high-dimensional classically entangled light, which allows control in a $2 \times 2 \times 2 \times 2 = 16$ dimensional space. The corresponding basis states are partially shown in Fig. 4(c) and fully shown in Supplement 1. Notably, the 16-dimensional classical entanglement is by no means a limitation, which can be further expanded with combination of more DoFs (polarization, time, etc [17, 18]).

In conclusion, we demonstrate a class of scalar structured light with multiple DoFs, which realizes full control of multipartite classically entangled states in high dimensions, in analogy with quantum entangled states with multiple particles. Specifically, we obtain a complete set of 8-dimensional tripartite classically entangled states, by exploiting the three DoFs (oscillating direction, roundtrip location and central OAM) of scalar RWGBs that are digitally generated and modulated by a SLM. Furthermore, we demonstrate four-partite 16-dimensional en-

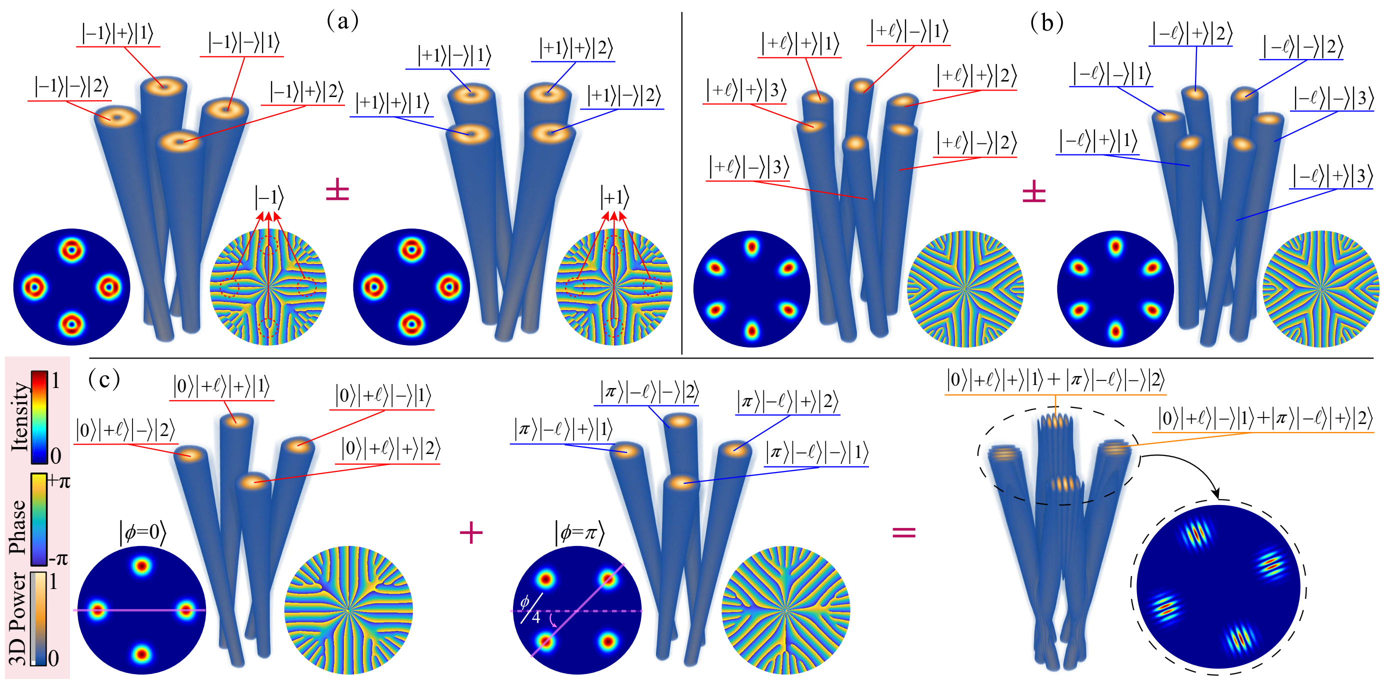

Fig. 4. Higher-dimensional classical entanglement formed by non-separable high-dimension multi-DoF scalar RWGBs. (a) Basis states with sub-OAM of $|\pm1\rangle$ in 8-dimensional space constructed by three DoFs, including sub-OAM, ray oscillating direction and roundtrip location; (b) basis states in 12-dimensional space by RWGBs with three roundtrip location states; (c) four-partite entangled states realized by four DoFs in RWGBs.

tanglement, by adding an intrinsic ray oscillating phase DoF of RWGBs. Our complete theoretical framework and digital realization method have offered an efficient and easy route for high dimensional optical manipulation, as well as extended applications in classical-quantum regimes.

Funding. This work was funded by National Natural Science Foundation of China (61975087).

Disclosures. The authors declare no conflicts of interest.

Data availability. Data underlying the results presented in this paper are not publicly available at this time but may be obtained from the authors upon reasonable request.

Supplemental document. See Supplement 1 for supporting content.

REFERENCES

1. A. Forbes, M. de Oliveira, and M. R. Dennis, Nat. Photonics **15**, 253 (2021).
2. M. McLaren, T. Konrad, and A. Forbes, Phys. Rev. A **92**, 023833 (2015).
3. V. D'Ambrosio, G. Carvacho, F. Graffitti, C. Vitelli, B. Piccirillo, L. Marrucci, and F. Sciarrino, Phys. Rev. A **94**, 030304 (2016).
4. A. Forbes, A. Aiello, and B. Ndagano, Prog. Opt. **64**, 99 (2019).
5. T. Konrad and A. Forbes, Contemp. Phys. **60**, 1 (2019).
6. A. Forbes, A. Aiello, and B. Ndagano, Prog. Opt. **64**, 99 (2019).
7. R. Ursin, F. Tiefenbacher, T. Schmitt-Manderbach, H. Weier, T. Scheidl, M. Lindenthal, B. Blauensteiner, T. Jennewein, J. Perdigues, P. Trojek, B. Ömer, M. Fürst, M. Meyenburg, J. Rarity, C. Barbieri, H. Weinfurter, and A. Zeilinger, Nat. Phys. **3**, 481 (2007).
8. G. Tóth and I. Apellaniz, J. Phys. A: Math. Theor. **47**, 424006 (2014).
9. S. Gröblacher, T. Jennewein, A. Vaziri, G. Weihs, and A. Zeilinger, New J. Phys. **8**, 75 (2006).
10. Y. Shen, I. Nape, X. Yang, X. Fu, M. Gong, D. Naidoo, and A. Forbes, Light. Sci. & Appl. **10**, 1 (2021).
11. R. Fickler, R. Lapkiewicz, M. Huber, M. P. Lavery, M. J. Padgett, and A. Zeilinger, Nat. Commun. **5**, 1 (2014).
12. W. Balthazar, C. Souza, D. Caetano, E. Galvão, J. Huguenin, and A. Khoury, Opt. Lett. **41**, 5797 (2016).
13. L. Chen, T. Ma, X. Qiu, D. Zhang, W. Zhang, and R. W. Boyd, Phys. Rev. Lett. **123**, 060403 (2019).
14. N. Korolkova and G. Leuchs, Reports on Prog. Phys. **82**, 056001 (2019).
15. Y. Shen, J. Opt. **23**, 124004 (2021).
16. Z. Wan, Z. Wang, X. Yang, Y. Shen, and X. Fu, Opt. Express **28**, 31043 (2020).
17. P. G. Kwiat, K. Mattle, H. Weinfurter, A. Zeilinger, A. V. Sergienko, and Y. Shih, Phys. Rev. Lett. **75**, 4337 (1995).
18. B. Brecht, D. V. Reddy, C. Silberhorn, and M. G. Raymer, Phys. Rev. X **5**, 041017 (2015).

FULL REFERENCES

1. A. Forbes, M. de Oliveira, and M. R. Dennis, "Structured light," Nat. Photonics **15**, 253–262 (2021).
2. M. McLaren, T. Konrad, and A. Forbes, "Measuring the nonseparability of vector vortex beams," Phys. Rev. A **92**, 023833 (2015).
3. V. D'Ambrosio, G. Carvacho, F. Graffitti, C. Vitelli, B. Piccirillo, L. Marrucci, and F. Sciarrino, "Entangled vector vortex beams," Phys. Rev. A **94**, 030304 (2016).
4. A. Forbes, A. Aiello, and B. Ndagano, "Classically entangled light," Prog. Opt. **64**, 99–153 (2019).
5. T. Konrad and A. Forbes, "Quantum mechanics and classical light," Contemp. Phys. **60**, 1–22 (2019).
6. A. Forbes, A. Aiello, and B. Ndagano, "Classically entangled light," Prog. Opt. **64**, 99–153 (2019).
7. R. Ursin, F. Tiefenbacher, T. Schmitt-Manderbach, H. Weier, T. Scheidl, M. Lindenthal, B. Blauensteiner, T. Jennewein, J. Perdigues, P. Trojek, B. Ömer, M. Fürst, M. Meyenburg, J. Rarity, C. Barbieri, H. Weinfurter, and A. Zeilinger, "Entanglement-based quantum communication over 144 km," Nat. Phys. **3**, 481–486 (2007).
8. G. Tóth and I. Apellaniz, "Quantum metrology from a quantum information science perspective," J. Phys. A: Math. Theor. **47**, 424006 (2014).
9. S. Gröblacher, T. Jennewein, A. Vaziri, G. Weihs, and A. Zeilinger, "Experimental quantum cryptography with qutrits," New J. Phys. **8**, 75 (2006).
10. Y. Shen, I. Nape, X. Yang, X. Fu, M. Gong, D. Naidoo, and A. Forbes, "Creation and control of high-dimensional multi-partite classically entangled light," Light. Sci. & Appl. **10**, 1–10 (2021).
11. R. Fickler, R. Lapkiewicz, M. Huber, M. P. Lavery, M. J. Padgett, and A. Zeilinger, "Interface between path and orbital angular momentum entanglement for high-dimensional photonic quantum information," Nat. Commun. **5**, 1–6 (2014).
12. W. Balthazar, C. Souza, D. Caetano, E. Galvão, J. Huguenin, and A. Khoury, "Tripartite nonseparability in classical optics," Opt. Lett. **41**, 5797–5800 (2016).
13. L. Chen, T. Ma, X. Qiu, D. Zhang, W. Zhang, and R. W. Boyd, "Realization of the einstein-podolsky-rosen paradox using radial position and radial momentum variables," Phys. Rev. Lett. **123**, 060403 (2019).
14. N. Korolkova and G. Leuchs, "Quantum correlations in separable multimode states and in classically entangled light," Reports on Prog. Phys. **82**, 056001 (2019).
15. Y. Shen, "Rays, waves, su (2) symmetry and geometry: toolkits for structured light," J. Opt. **23**, 124004 (2021).
16. Z. Wan, Z. Wang, X. Yang, Y. Shen, and X. Fu, "Digitally tailoring arbitrary structured light of generalized ray-wave duality," Opt. Express **28**, 31043–31056 (2020).
17. P. G. Kwiat, K. Mattle, H. Weinfurter, A. Zeilinger, A. V. Sergienko, and Y. Shih, "New high-intensity source of polarization-entangled photon pairs," Phys. Rev. Lett. **75**, 4337–4341 (1995).
18. B. Brecht, D. V. Reddy, C. Silberhorn, and M. G. Raymer, "Photon temporal modes: A complete framework for quantum information science," Phys. Rev. X **5**, 041017 (2015).